7-2009

Pseudomorphic stabilization of rocksalt GaN in TiN/GaN multilayers and superlattices

Vijay Rawat
Purdue University - Main Campus, vijay.rawat@gmail.com

Dmitri Zakharov
Purdue University - Main Campus, zakharov@purdue.edu

E A. Stach
Birck Nanotechnology Center and School of Materials Engineering, Purdue University, eastach@purdue.edu

Timothy D. Sands
Purdue University, tsands@purdue.edu

Pseudomorphic stabilization of rocksalt GaN in TiN/GaN multilayers and superlattices

Vijay Rawat,[1,2,3,*] Dmitri N. Zakharov,[3] Eric A. Stach,[1,3] and Timothy D. Sands[1,2,3]
[1]*School of Materials Engineering, Purdue University, West Lafayette, Indiana 47907, USA*
[2]*School of Electrical and Computer Engineering, Purdue University, West Lafayette, Indiana 47907, USA*
[3]*Birck Nanotechnology Center, Purdue University, West Lafayette, Indiana 47907, USA*
(Received 20 February 2009; revised manuscript received 24 May 2009; published 22 July 2009)

Gallium nitride (GaN) in its stable wurtzite phase has proven its utility in light-emitting diodes and diode lasers as well as high-temperature and high-power electronic devices. In addition to its equilibrium wurtzite phase, GaN exhibits two cubic polymorphs, a zinc-blende phase and a high-pressure rocksalt phase. Here, we report the pseudomorphic stabilization of the high-pressure rocksalt phase of GaN within TiN/GaN multilayers as verified using x-ray diffraction and high-resolution transmission electron microscopy. High-resolution lattice imaging confirmed that the lattice parameter of the rocksalt GaN phase is 0.41 nm. The critical thickness of the GaN film that can be pseudomophically stabilized in rocksalt phase within TiN/GaN superlattices is determined to be less than 2 nm.

DOI: 10.1103/PhysRevB.80.024114 PACS number(s): 64.60.My, 68.37.Og, 62.23.Pq

I. INTRODUCTION

During thin-film growth, it is possible to stabilize bulk metastable phases in thin-film form during epitaxial growth on substrates with crystal structure and lattice parameters that are similar to those of the metastable phase. This pseudomorphic stabilization has been observed in a wide range of materials systems.[1–3] Such growth strategies have enabled stabilization of phases that are typically observed only at elevated temperatures and/or pressures. All of the semiconductors belonging to the III–V nitride family (e.g., GaN, AlN, and InN) exhibit the hexagonal wurtzite crystal structure in equilibrium at low pressures while cubic phases are stabilized when grown under high-pressure conditions.[4–7] The rocksalt phase has been theoretically shown to have markedly different electrical, optical, and phonon characteristics than the wurtzite phase. The cubic zinc-blende phase of Gallium nitride (GaN) has been grown along with the wurtzite phase by organometallic vapor-phase epitaxy, molecular beam epitaxy, and radio-frequency magnetron sputtering processes;[3,8–13] however, the metastable rocksalt phase has not been grown in thin-film form. Nanoparticles of GaN with the rocksalt crystal structure have been synthesized using solvothermal techniques but other possible compounds of gallium were also observed to be present.[14] The transition of the wurtzite phase to the rocksalt phase has been observed in GaN films when they are subjected to high hydrostatic pressures (pressure >50 GPa) in diamond-anvil cells.[15] Similar wurtzite-to-rocksalt transitions at high pressures have also been observed in AlN and InN.[16] Pseudomophic stabilization of the rocksalt phase using closely lattice-matched metallic underlayers has been reported previously in the case of AlN in TiN/AlN and VN/AlN superlattices.[17,18] It is more difficult to grow GaN in the rocksalt crystal structure as compared to AlN or InN due to a larger difference in the free energies of formation of the rocksalt phase and the wurtzite phase at ambient pressure.[7,19] It has been observed experimentally that the wurtzite-to-rocksalt transition in the case of GaN in diamond-anvil cells requires a hydrostatic pressure of 52 GPa which is considerably higher than that for the similar transition in AlN ($\sim$13 GPa).[7,20,21]

In an earlier study of TiN/GaN multilayers by two of the authors,[22] x-ray diffraction patterns provided indirect evidence for the stabilization of rocksalt GaN for GaN layer thicknesses of $\sim$1 nm. In the present work, we report an extensive x-ray diffraction and high-resolution transmission electron microscopy (TEM) study of the multilayers, confirming the pseudomorphic stabilization of the rocksalt GaN (rs-GaN) phase. Additionally, we determine experimentally the approximate critical thickness at which this phase transforms to its equilibrium wurtzite structure. These rocksalt-structured TiN/GaN metal/semiconductor superlattices represent a class of metamaterials that are likely to exhibit highly anisotropic optical, electronic, and thermal properties that could find application in solid-state thermionic-energy converters, photodetectors, nanoplasmonics, and photothermal-energy conversion devices.

II. EXPERIMENTAL DETAILS

TiN/GaN multilayers were grown using reactive pulsed-laser deposition (KrF laser, 248 nm) on MgO substrates. The ammonia-gas pressure during growth was 20 mtorr while the substrates were maintained at a temperature of 580 °C, measured using an infrared pyrometer.[22] The comparable surface energies of TiN and GaN, a low homologous epitaxial-growth temperature and similar lattice parameters allowed the growth of coherent TiN/rs-GaN superlattices with large numbers of periods. The period of the multilayers was measured using Rutherford backscattered spectrometry (RBS) performed at Thin Film Analysis Inc. (Santa Clara, CA) using a General Ionex Model 5110 with a 1 MV Tandem Accelerator. The RBS spectra were analyzed using DETECTOR™ software developed by MeV Technologies, Inc. The rocksalt TiN and rocksalt GaN areal atomic density per unit thickness were calculated from their respective volumetric atomic densities and were compared with the RBS measured areal atomic densities to determine the relative thicknesses of TiN and GaN in the multilayers. The number of periods was used to determine the TiN- and GaN-layer thicknesses. The accuracy of this technique for measuring nanoscale periods have

TABLE I. Periods and layer thicknesses of TiN/GaN multilayers determined using RBS.

Sample	Number of periods	RBS equivalent total film thickness (μm)	TiN/GaN-layer thicknesses and total period thicknesses
A	980	2.35	1.4 nm/1 nm (2.4 nm)
B	260	1.05	2.8 nm/1.2 nm (4 nm)
C	280	1.32	3.2 nm/1.5 nm (4.7 nm)
D	154	0.814	3.7 nm/1.6 nm (5.3 nm)
E	182	1.01	4.4 nm/1.2 nm (5.6 nm)
F	60	1.10	12.2 nm/6.2 nm (18.4 nm)

been demonstrated in a prior publication.[24] X-ray diffraction studies of the multilayers were performed using Cu $K\alpha$ radiation in a Panalytical X'pert diffractometer equipped with a four-crystal Ge monochromator on the incident x-ray beam side. High-resolution electron microscopy was performed using an FEI Titan 80/300 operating at 300 kV. Bright field-diffraction contrast images and microdiffraction patterns were obtained with a JEOL 2000FX operating at 200 kV.

Six different TiN/GaN multilayers with increasing period thicknesses were grown on (100) rocksalt MgO substrates. A 50-nm-thick TiN buffer layer was grown on the MgO substrate before starting the growth of the multilayer. MgO substrates (rocksalt, $a=0.42$ nm) were chosen as they have a similar crystal structure and close lattice match with the TiN (rocksalt, $a=0.424$ nm) buffer layer. The periods of the multilayers, as determined by RBS, are listed in Table I.

Figure 1 shows the x-ray ω-2θ scans obtained from the multilayers and depicts the evolution of the wurtzite GaN phase with increasing period. The rocksalt phase of GaN, when grown epitaxially on a (100)-oriented TiN film, shows a 200 reflection that is close to or overlapping the TiN 200 reflection. The presence of the wurtzite phase is indicated by the appearance of one or more of the three high-intensity wurtzite reflections corresponding to the $\{10\bar{1}0\}$, $\{0002\}$, and $\{10\bar{1}1\}$ families of planes. X-ray diffraction patterns from the thinner period samples, i.e., samples A–D, do not show any peak from the wurtzite GaN phase and the shift in the TiN 200 reflection with increasing period suggests that the rs-GaN 200 reflection is overlapping the TiN 200 reflection.

Additionally, the diffraction pattern of sample D shows evenly spaced interference peaks corresponding to a period of 5.6 nm, which matches well with the period of 5.3 nm inferred from the RBS measurement. X-ray patterns from sample D also showed two broad peaks corresponding to TiN 200 and rs-GaN 200 reflections. The broad peaks suggest coherently strained TiN and rs-GaN layers. The crossplane lattice parameter for the strained TiN layer varies in the range 0.42–0.43 nm while that for rsGaN varied in the range of 0.40–0.41 nm. Only the diffraction pattern from the thickest period sample, sample F, shows the presence of the wurtzite GaN (wz-GaN) phase.

Samples D and F were analyzed using cross-sectional transmission electron microscopy (Figs. 2 and 3, respectively). The lattice image of sample F shows that the first two

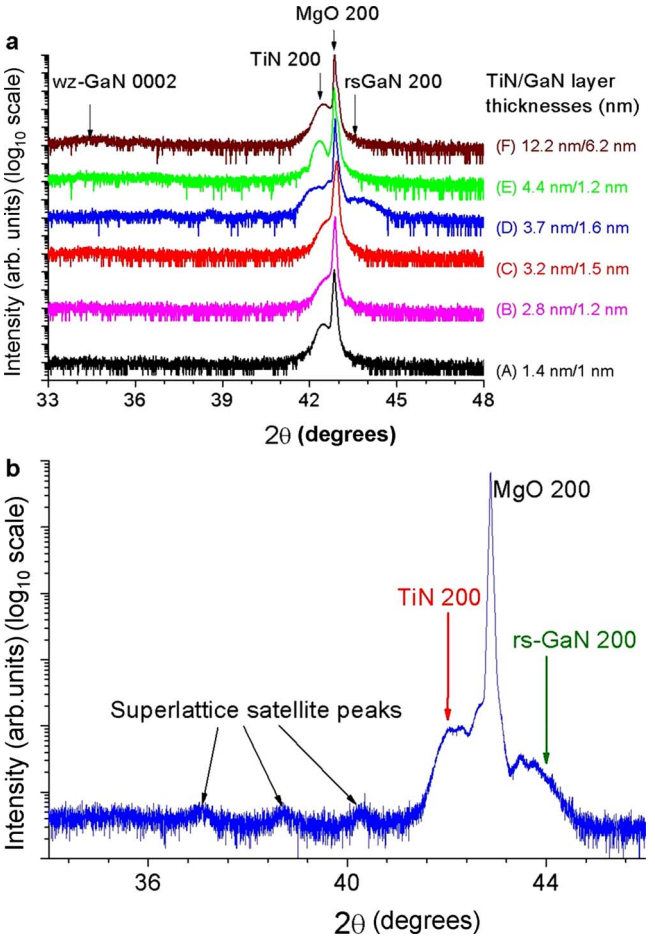

FIG. 1. (Color online) (a) X-ray diffraction patterns from six TiN/GaN multilayers with varying period thicknesses showing the presence of the wz-GaN phase in the sample with the largest period. (b) A high-resolution diffraction pattern from sample D shows satellite peaks with their spacing matching the period thickness of the multilayer.

layers of GaN are epitaxial with lattice fringes that are consistent with the rocksalt structure. The fast Fourier transform (FFT) diffractograms created from the image of the first two GaN layers in the multilayer are also shown in Fig. 2 and they are consistent with the conclusion that the GaN layers are cubic. Using the lattice parameter of the MgO substrate as reference, the strained in-plane and crossplane lattice parameters for the cubic GaN phase were measured from the TEM lattice image to be $a_{\parallel}=0.412\pm0.032$ nm and $a_{\perp}=0.406\pm0.014$ nm. These values are consistent with a relaxed rocksalt lattice parameter of $a=0.41$ nm, which matches well with the value reported in the literature.[15] The measured in-plane and crossplane lattice parameters confirm that the cubic phase adopts the rocksalt structure of GaN and not the zinc-blende structure, which has a lattice parameter of 0.45 nm. Similarly, the cross-sectional lattice image from sample D confirms the presence of a superlattice structure and the FFT diffractogram obtained from the whole sample confirms that the cubic structure is retained throughout the cross section of the superlattice. The relaxed lattice parameter of the rocksalt GaN phase in this sample was measured to be 0.41 nm.

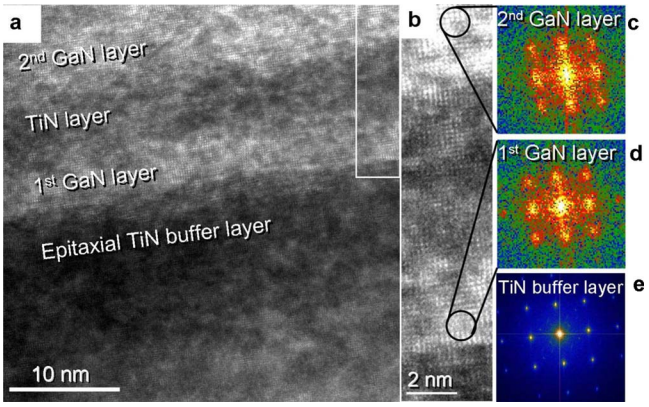

FIG. 2. (Color online) High-resolution cross-sectional TEM image of TiN (12.2 nm)/GaN (6.2 nm) multilayer grown on MgO (100) substrate. (a) The lattice image shows the cube-on-cube epitaxy of GaN layers on TiN layers; (b) inset in the middle shows a magnified view of the lattice image; (right), the comparison of the FFT patterns obtained from the GaN layers [(c) and (d)] with the one obtained from TiN buffer layer (e) confirms the cubic crystal structure of the epitaxial GaN phase.

Since the TiN buffer layer (50 nm) is much thicker than the first GaN layer (~6 nm), it can be assumed that most of the mismatch strain is accommodated by the GaN layer. The measured in-plane lattice parameters of rs-GaN and TiN suggest a 2% in-plane biaxial tensile strain in the GaN layer if the rs-GaN layer is coherent. This lattice misfit is expected to be partly accommodated by the introduction of dislocations with Burgers vectors that have edge components in the plane of the interface. With an increase in the thickness of the GaN layer, the free energy (residual lattice-mismatch strain, misfit dislocation, and volume-free energy terms) per unit area of the interface increases until it becomes energetically favorable for the rs-GaN to transform to the wurtzite phase. It is expected that the experimentally determined critical thickness for this transition will exceed the equilibrium critical thickness by an amount that depends on temperature, density,

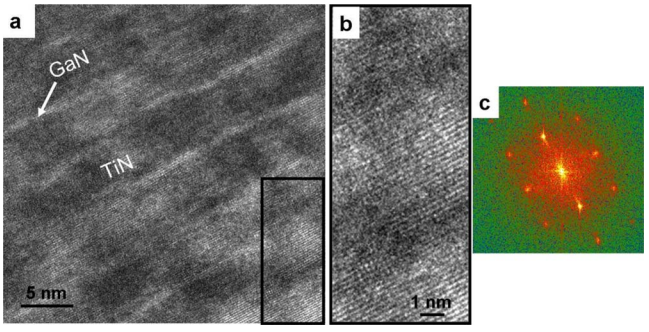

FIG. 3. (Color online) High-resolution cross-sectional TEM image of TiN(3.7 nm)/GaN(1.6 nm) superlattice grown on an MgO(100) substrate. (a) The lattice image obtained from the middle of the sample confirming the existence of a superlattice structure; (b) a magnified view of the lattice image showing the cube-on-cube epitaxy throughout the superlattice; and (c) the FFT pattern obtained from the leftmost image confirming the cubic symmetry throughout the cross section of the multilayer sample.

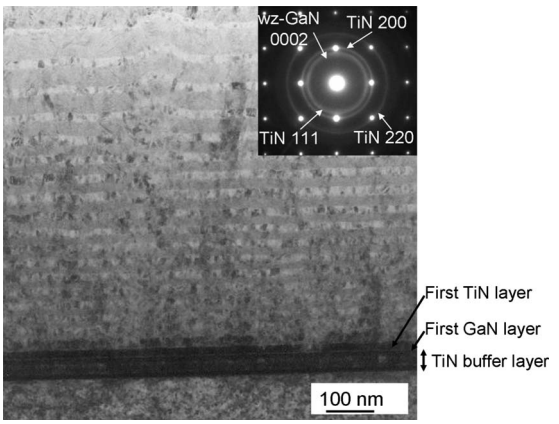

FIG. 4. Cross-sectional TEM image of a TiN(20 nm)/GaN(variable thickness) multilayer grown on MgO(100). Cross-sectional TEM image of a TiN/GaN multilayer in which the TiN-layer thickness is kept constant at 20 nm while the GaN-layer thickness is systematically increased from 1.5 to 50 nm in order to determine the critical thickness at which the rocksalt-to-wurtzite transformation takes place in the GaN layers. The image shows that the interface between the first TiN and the first GaN layer is sharp and the interface roughness increases with increase in thickness of GaN layer. (Inset) Selected area diffraction pattern obtained from the multilayer and the MgO substrate showing that the multilayer is composed of polycrystalline layers.

and character of extended defects such as dislocations, stacking faults, and the interface step structure. Nevertheless, an experimental measurement will give an upper bound for the equilibrium critical thickness for pseudomorphic stabilization. It is important to note that the equilibrium critical thickness for the rocksalt-to-wurtzite phase transition is a function of the lattice mismatch between rocksalt GaN and its rocksalt substrate (TiN in this study). A smaller lattice mismatch will result in a larger critical thickness, as has been observed in a prior studies of the stabilization of rocksalt AlN in TiN/AlN and VN/AlN superlattices.[19,20] Based on samples D and F alone, it can be concluded that the experimental critical thickness for rs-GaN phase under these growth conditions is between 1.6 and 6.2 nm. Although the first two GaN layers in sample F adopt the rocksalt structure, subsequent layers have relaxed to the wurtzite phase.

In order to refine the determination of an experimental critical thickness, a TiN/GaN multilayer was grown in which the TiN-layer thickness was kept constant at 20 nm while the GaN thickness was systematically increased from 1.5 to 50 nm. Figure 4 shows a low magnification cross-sectional TEM image from the sample showing that the bottom few layers of the multilayer are very flat and of different contrast than the remainder of the GaN layers, suggesting that the first few GaN layers are pseudomorphic. The inset shows the selected area diffraction pattern obtained from the cross section of the whole sample (substrate as well as the multilayer) showing that the multilayer is polycrystalline. A higher magnification image of the same sample is shown in Fig. 5(a). Microdiffraction was employed to determine the crystal structure of each GaN layer. Figures 5(b)–5(d) show microdiffraction patterns obtained from the MgO substrate, the

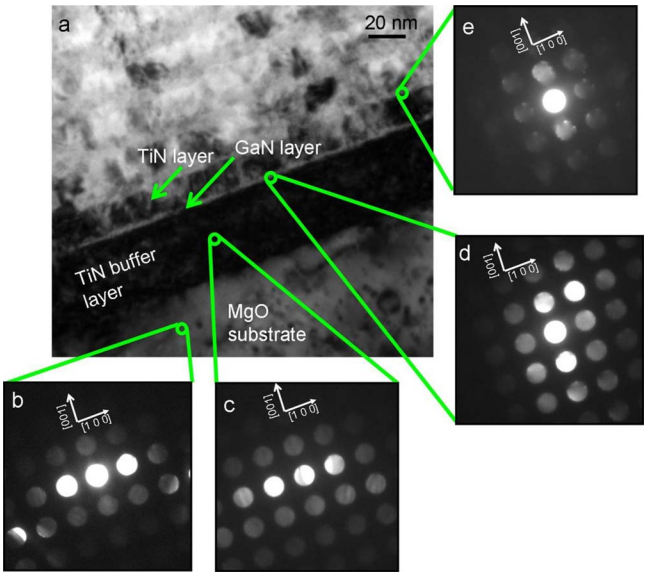

FIG. 5. (Color online) Microdiffraction patterns obtained from different layers of the TiN (20 nm)/GaN (variable thickness) multilayer. (a) Cross-sectional TEM image showing the bottom layers of TiN(20 nm)/GaN(variable thickness) multilayer grown on MgO (100) substrate. ⟨010⟩ zone axis electron-beam microdiffraction pattern obtained from the (b) MgO substrate, (c) TiN buffer layer, (d) the first GaN layer (~1.5–2 nm), and (e) the second GaN layer (~1.5–2 nm). The microdiffraction patterns confirm that the cubic symmetry of the MgO substrate is retained in the TiN buffer layer and in the first two GaN layers.

TiN buffer layer, and the two initial GaN layers of 1.5–2 nm thickness, respectively. As can be seen from the microdiffraction patterns, the cubic symmetry of the MgO substrate was sustained in the GaN layers and the comparison of spacings between the 200 and 220 reflections from the GaN layer with the reflections from the MgO diffraction pattern confirmed that the first two GaN layers adopted the rocksalt structure. Microdiffraction from the third GaN layer exhibited additional reflections, suggesting the presence of the wz-GaN phase. Thus, considering these results along with the data from sample D, the experimental critical thickness for rs-GaN films when grown on (100)-oriented TiN films is in the range of 1.5–2 nm. It must be emphasized that measured values of critical thickness are expected to be equal to or larger than the equilibrium critical thickness as determined by the role of kinetic barriers to relaxation of the pseudomorphic rocksalt GaN layers.

III. CONCLUSION

In summary, GaN has been stabilized in the rocksalt phase in pseudomorphic layers grown on rocksalt-structured (100)-oriented TiN films. The experimental critical thickness is determined to be less than 2 nm but improved lattice matching between rs-GaN film and the rocksalt-structured substrate or underlayer should increase the critical thickness. The high-pressure rs-GaN phase is expected to exhibit substantially different electronic and optical properties than those of the equilibrium wurtzite phase.[23,24] Electronic-structure calculations of rs-GaN have indicated that the phase has an indirect bandgap of 1.7 eV with valence-band maxima at the *L* points and a conduction-band minimum along the *X*-*W* direction, unlike the other two polymorphs of GaN that are direct bandgap semiconductors. The controlled synthesis of the rocksalt phase of GaN in thin-film form may enable experimental determination and verification of properties hitherto only theoretically predicted. Furthermore, fabrication of superlattices of metal and semiconductor combinations, which have the desired Schottky barrier heights and show reduction in thermal conductivity, are important specifically for the area of solid-state thermionic energy conversion.[25]

ACKNOWLEDGMENTS

This work was supported by ONR/DoD through a multidisciplinary university research initiative (MURI) grant to the Thermionic Energy Conversion Center. A part of this work was carried out in the Center for Microanalysis of Materials, University of Illinois, which is partially supported by the U.S. Department of Energy under Grant No. DEFG02-91-ER45439.

*Corresponding author; Present address: 2213 Mclaughlin Ave, #1, San Jose, CA 95122. FAX: 408-717-9073; vrawat@purdue.edu

[1] W. Kummerle and U. Gradmann, Solid State Commun. **24**, 33 (1977).
[2] G. A. Prinz, Phys. Rev. Lett. **54**, 1051 (1985).
[3] M. Baleva and E. Mateeva, J. Phys.: Condens. Matter **5**, 7959 (1993).
[4] F. A. Ponce and D. P. Bour, Nature (London) **386**, 351 (1997).
[5] S. Nakamura and G. Fasol, *The Blue Laser Diode.: GaN based Light Emitters and Lasers*, (Springer-Verlag, New York, 2001).
[6] S. Strite and H. Morkoc, J. Vac. Sci. Technol. B **10**, 1237 (1992).
[7] S. Uehara, T. Masamoto, A. Onodera, M. Ueno, O. Shimomura, and K. Takemura, J. Phys. Chem. Solids **58**, 2093 (1997).
[8] A. Nakadaira and H. Tanaka, J. Electron. Mater. **26**, 320 (1997).
[9] J. G. Kim, A. C. Frenkel, H. Liu, and R. M. Park, Appl. Phys. Lett. **65**, 91 (1994).
[10] M. E. Lin, G. Xue, G. L. Zhou, J. E. Greene, and H. Morkoc, Appl. Phys. Lett. **63**, 932 (1993).
[11] Y. Zhao, C. W. Tu, I. T. Bae, and T. Y. Seong, Appl. Phys. Lett. **74**, 3182 (1999).
[12] J. H. Kim and P. H. Holloway, Appl. Phys. Lett. **84**, 711 (2004).
[13] C. G. Zhang, L. F. Bian, W. D. Chen, and C. C. Hsu, J. Cryst. Growth **299**, 268 (2007).
[14] F. Xu, Y. Xie, X. Zhang, S. Zhang, and L. Shi, New J. Chem. **27**, 565 (2003).
[15] M. Ueno, M. Yoshida, A. Onodera, O. Shimomura, and K. Takemura, Phys. Rev. B **49**, 14 (1994).

[16] A. Munoz and K. Kunc, Phys. Rev. B **44**, 10372 (1991).
[17] A. Madan, I. W. Kim, S. C. Cheng, P. Yashar, V. P. Dravid, and S. A. Barnett, Phys. Rev. Lett. **78**, 1743 (1997).
[18] Q. Li, I. W. Kim, and S. A. Barnett, J. Mater. Res. **17**, 1224 (2002).
[19] J. Serrano, A. Rubio, E. Hernandez, A. Munoz, and A. Mujica, Phys. Rev. B **62**, 16612 (2000).
[20] N. E. Christensen and I. Gorczyca, Phys. Rev. B **50**, 4397 (1994).
[21] P. Zapol, R. Pandey, and J. D. Gale, J. Phys.: Condens. Matter **9**, 9517 (1997).
[22] V. Rawat and T. D. Sands, J. Appl. Phys. **100**, 064901 (2006).
[23] R. Laskowski and N. E. Christensen, Phys. Status Solidi B **244**, 17 (2007).
[24] Z. W. Chen, M. Y. Lv, L. X. Li, Q. Wang, X. Y. Zhang, and R. P. Liu, Thin Solid Films **515**, 2433 (2006).
[25] V. Rawat, Y. K. Koh, D. Cahill, and T. D. Sands, J. Appl. Phys. **105**, 024909 (2009).